Cellular and Molecular Bioengineering (© 2021)
https://doi.org/10.1007/s12195-020-00665-6

BMES BIOMEDICAL ENGINEERING SOCIETY

Methods Paper

Droplet Microfluidics with Reagent Micromixing for Investigating Intrinsic Platelet Functionality

MAAIKE S. A. JONGEN,[1,2] PAUL M. HOLLOWAY,[2,3] SIMON I. R. LANE,[4] NICOLA A. ENGLYST,[2,5] OWEN J. T. MCCARTY,[1] and JONATHAN WEST[2,5]

[1]Department of Biomedical Engineering, School of Medicine, Oregon Health and Science University, Portland, OR, USA; [2]Faculty of Medicine, University of Southampton, Southampton SO17 1BJ, UK; [3]Investigative Medicine Division, Radcliffe Department of Medicine, University of Oxford, Oxford OX3 9DU, UK; [4]Faculty of Engineering and Physical Sciences, University of Southampton, Southampton SO17 1BK, UK; and [5]Institute for Life Sciences, University of Southampton, Southampton SO17 1BJ, UK

(*Received 18 August 2020; accepted 23 December 2020*)

Associate Editor Michael R. King oversaw the review of this article.

Abstract

Introduction—Precision mapping of the functional structure of platelet populations holds great promise for the identification of hyper-reactive subtypes that are likely to be disease drivers, having value in prognostics and as therapeutic targets. However, the ability to measure the intrinsic functional capacity of individual platelets is confounded by potent paracrine cross-talk, resulting in phenotypic remodeling of the entire platelet population, and in doing so obscuring the identity of hyper-reactive platelets.

Methods—To address this we have developed a droplet microfluidics strategy for single platelet confinement to exclude paracrine signaling. Consideration of the Poisson distribution was used for high throughput single platelet encapsulation and the preparation of minimal platelet collectives serving as digital models for understanding the role of hyper-reactive platelets coordinating system-level behavior by paracrine signaling. Platelets are retrieved from the droplets for phenotyping using standard flow cytometry. In addition, we have incorporated a staggered herringbone micromixing element for accurate agonist and antibody dispensing in droplets.

Results—The methodology was used for characterizing sensitivity distributions from healthy blood donors in response to convulxin (agonist of the GPVI receptor, the major platelet receptor for collagen). P-selectin exposure and $\alpha_{IIb}\beta_3$ integrin activation were used as analytical end-points to demonstrate the existence of hyper-reactive platelets that direct 20-fold gains in system level sensitivity.

Conclusions—The analytical workflow represents an enabling tool for the accurate classification of platelet subtypes and description of their underlying biology.

Keywords—Platelets, Single cell analysis, Droplet microfluidics, Micromixing, Flow cytometry.

ABBREVIATIONS

PDMS	Poly(dimethylsiloxane)
PRP	Platelet rich plasma
HEPES	Sodium 2-(4-(2-hydroxyethyl)piperazin-1-yl)ethanesulfonate
BSA	Bovine serum albumin
CVX	Convulxin
PBS	Phosphate buffered saline

INTRODUCTION

Platelets respond to blood vessel damage for coordinated repair, but also play a critical role in cardiovascular disease. Platelet functional diversity has long been a matter of investigation[5,21] with the enticing possibility of identifying a platelet subtype that drives pathophysiological thrombus formation, a prognostic marker for risk of heart attacks and strokes and a choice therapeutic target.[2,6,13,21] Key examples are immature, so-called reticulated platelets, distinguished by volume and elevated RNA content correlating with

Address correspondence to Jonathan West, Faculty of Medicine, University of Southampton, Southampton SO17 1BJ, UK. Electronic mail: j.j.west@soton.ac.uk

Maaike S. A. Jongen, Paul M. Holloway, and Simon I. R. Lane have contributed equally to this work.

disease[3,10] and the identification of pro-aggregatory and pro-coagulant heterotypic states emerging following dual stimulation with collagen and thrombin.[1,17] However, definitive platelet function measurements requires stimulation, leading to potent paracrine signaling driving the activation of otherwise unreactive platelets and obscuring the classification of hyper-reactive platelets from less reactive, 'follower' platelets. Methods are therefore needed to compartmentalize single platelets to prevent paracrine cross-talk and preserve their intrinsic functional capacity. Microfluidic methods are suited for single cell manipulations,[14] with droplet microfluidics[23] being the preferred approach for high throughput encapsulations to enable large-scale screening campaigns.[7] In this contribution, we build on the first demonstration of droplet microfluidics for investigating single platelet functional variability[9] by providing a detailed description of the droplet confinement approach and the inclusion of a micromixer element for assay reliability and automation.

DROPLET MICROFLUIDICS

Droplet microfluidic devices were prepared using the standard SU-8 to PDMS soft lithography route. Inlet and outlet ports were introduced using a 1-mm-diameter biopsy punch (Miltex) and Scotch® Magic™ Tape (3M™, 810) was used to remove any particulates. Oxygen plasma bonding (Femto, Deiner) was used to secure the PDMS (Sylgard 184) channels to a microscope slide acting both as a window and handle. The microscope slide can be coated with a thin film of PDMS or used in its native state for plasma bonding. Following assembly, devices were flooded from the outlet with 1% (v/v) trichloro(1*H*,1*H*,2*H*,2*H*-perfluorooctyl)silane (Merck) in HFE-7500™ (3M™) to passivate the PDMS and glass surfaces. This ensures partitioning of the fluoro-oil phase to the microchannel walls for the reliable generation of monodisperse droplets. In addition, glass surfaces activate platelets,[15,22] but the passivation of the *glassy-like* plasma activated PDMS and glass surfaces with the fluorinated silane prevents direct platelet contact and activation. For droplet generation experiments, 0.75% (v/v) 008-fluorosurfactant (RAN Biotechnologies) was added to a HFE-7500™ carrier fluoro-oil. The surfactant is a non-ionic tri-block copolymer of poly(ethylene glycol) (PEG) and perfluoropolythene (PFPE) which stabilizes aqueous-fluoro-oil emulsions and is biocompatible, preventing the adsorption and interaction of biomolecules at the droplet interface.[8]

Microchannels were fabricated to a height of 20 μm. Passive filters having 15-μm-gaps between structures were placed downstream of the fluoro-oil, agonist and antibody inlets to reduce particle and fibre fouling, prolonging reliable device operation. The pinched droplet generation junction had a width of 22 μm, abruptly expanding to 50 μm for the generation of picolitre droplets. Droplet size can be modulated by shear rate (velocity) and also the fluoro-oil:aqueous flow ratio. In practice, a 4:1 ratio was used involving the delivery of 20 μL/min fluoro-oil-surfactant with 2 μL/min of both agonist and antibody solutions and 1 μL/min platelet suspensions. Having independent platelet and antibody inputs prevents extravagant antibody consumption and is necessary to attain optimal flow cytometry signal to noise levels (see Electronic Supplementary Material, ESM Fig. 1). Samples and reagents were housed in syringes bearing 25G needles and interfaced to the microfluidic device using medical grade, sterile polythene tubing (ID 0.38 mm; OD 1.09 mm). This tubing is tightly secured over the needle and, by straightforward insertion, fits securely within the microfluidic ports (prepared using the 1-mm-diamater biopsy punch). Flow rates were managed using syringe pumps (Fusion 200, Chemyx). Droplet generation was imaged using a high-speed camera (2500 fps, Miro eX2, Phantom) to allow real-time quality control analysis, necessary to ensure flows had stabilised for the reliable generation of monodisperse droplets before collection for downstream analysis. The flow arrangements for monodisperse droplet generation are shown in Figs. 1a and 1b allowing the generation of monodisperse 25-μm-diameter droplets (CV±0.95%) with a volume of ~8 pL at a frequency of 10.4 kHz (Figs. 1c and 1d). Platelets are characteristically shear sensitive.[11] These conditions produce a junction mean flow velocity of ~1 m/s, imparting shear rates and stresses which exceed physiological conditions.[20] Critically, however, junction transit times are of the order ~50 μs, with droplets exiting the device within 20 ms. These shear durations are insufficient for platelet activation as evidenced using vehicle controls.

ENCAPSULATION STATISTICS

Platelets are near neutrally buoyant, remaining in suspension throughout experimental durations. This allows the continuous delivery of platelets to the microfluidic device for encapsulation within droplets. Unlike other cells which appreciably sediment this avoids the requirement for stirring mechanisms[12] which pose the risk of inadvertent platelet activation. Platelets are delivered randomly, requiring consideration of the Poisson statistic for controlled platelet encapsulation. The probability of platelets being encapsulated in a droplet is described as follows;

Journal : CMBE MS Code : 12195 PIPS No. : 665 ☐ TYPESET ☑ DISK ☐ LE ☑ CP Dispatch : 13-1-2021 Pages : 8

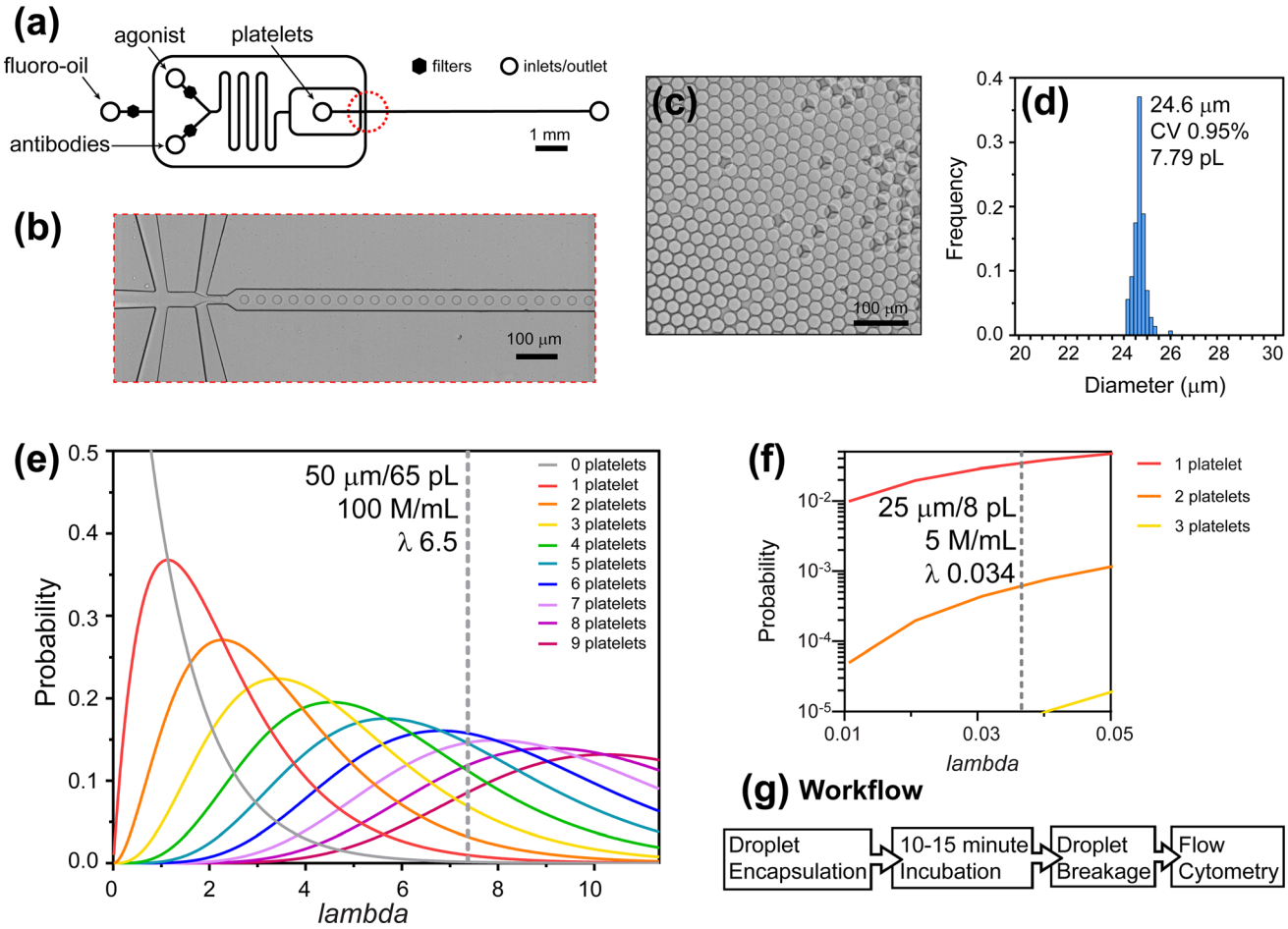

FIGURE 1. Microfluidics and Poisson distribution considerations for platelet encapsulation in droplets. Microfluidic device layout with aqueous and oil inputs and droplet generation junction identified with a red dashed circle (a). Droplets generated at 10.4 kHz (b) and resulting monodisperse droplets (c) with ImageJ-based size analysis involving >1000 droplets (d). Poisson distribution probabilities for given λ values to define encapsulation conditions for platelets with chosen λ = 6.5 conditions for multi-platelet encapsulation highlighted with a grey dashed line (e). Single platelet encapsulation probabilities (note $\log_{10}$ *y*-axis scaling) with chosen λ = 0.034 conditions for single platelet encapsulation highlighted with a grey dashed line (f). Overall workflow for measuring single platelet intrinsic functional capacity (g). Figure elements adapted from Jongen *et al*[9] (CC BY 4.0)

$$P_{(X)} = \frac{\lambda^{X} e^{-\lambda}}{X}$$

where $P_{(X)}$ is the probability of X number of platelets being packaged in a droplet and λ the mean number of platelets per droplet. For the encapsulation of single platelets in the ~8 pL droplets we used a conservative platelet input concentration of 25 × 10^6/mL, that is diluted 5-fold upon combination with agonist and antibody streams. This yields a λ value of 0.034, or 3.34% of droplets containing a single platelet, 0.08% containing multiples and with the majority of droplets empty. In this case, single platelet encapsulations outnumbered multiple platelet encapsulations 42-fold, with flow cytometric forward scatter area vs height gating used to further exclude platelet multiples (aggregating upon activation) from analysis. Single platelet encapsulation eliminates paracrine cross-talk, but this at the expense of throughput. A strength of droplet microfluidics is the kHz droplet generation rates, so even with >96% empty droplets, >100,000 single platelets can be encapsulated in 5 min, sufficient to effectively survey diversity in the platelet population.

In addition to using droplets to measure single platelet intrinsic functionality, the analysis of small platelet collectives has value for understanding the role of paracrine cooperativity: The presence of a single hypersensitive platelet in confinement is sufficient to activate other platelets in the same droplet, whereas the absence of hypersensitive platelets in a droplet prevents the platelets from being activated. In doing so, a digital responsive:unresponsive pattern is observed when analysing the droplets by fluorescent microscopy. For the preparation of small, minimal collectives the droplet microfluidics device was up-scaled with a 50×50 μm droplet generation junction and operation using 80

Journal : CMBE MS Code : 12195 PIPS No. : 665 ☐ TYPESET ☑ DISK ☐ LE ☑ CP Dispatch : 13-1-2021 Pages : 8

μL/min fluoro-oil, 4 μL/min undiluted PRP (~5×10^8/mL), and 8 μL/min agonist and antibody flows. This produced 50-μm-diameter droplets (CV±0.89%), with the 65 pL volume (and dilution by reagents) leading to a μ value of 6.5, or 0–15 platelets per droplet. Poisson distribution theory and the described single and multiple platelet encapsulation conditions are described in Figs. 1e and 1f.

PLATELET SENSITIVITY MEASUREMENTS

Controlled platelet encapsulation requires a platelet count during sample preparation. This was achieved using a method involving platelet-specific CD61 antibody labelling for analysis using an Accuri C6 (BD Biosciences) instrument.[16] The overall sampling process involved obtaining blood from healthy volunteers (free from anti-platelet medication) with informed consent and ethical approvals. Wide-bore venepuncture using a 21G needle was used to collect blood (with the first 4 mL discarded) into vacuum tubes containing 1:10 v/v 3.2% trisodium citrate. Gentle tube inversion was followed by centrifugation at 240 g for 15 min without brake for the preparation of PRP that was rested for 30 min before experiments. Using the platelet count, the PRP was adjusted to a final concentration of 25 × 10^6/mL in HEPES buffer (136 mM NaCl, 2.7 mM KCl, 10 mM HEPES, 2 mM $MgCl_2$, 0.1% (w/v) glucose and 1% (w/v) BSA (pH 7.45) for single platelet measurements or left undiluted for the minimal collective measurements.

The overall analytical workflow involved the encapsulation of single platelets with agonist and fluorescent reporter antibodies in droplets, followed by incubation, then releasing and fixing the platelets for flow cytometry (Fig. 1g). Platelets were stimulated with the potent platelet agonist convulxin (CVX, (Enzo Life Sciences) a snake venom toxin serving as a soluble proxy for ECM proteins including collagen that activate platelets via the GPVI receptor[4,18] to drive global platelet activation with notable end-points being $\alpha_{IIb}\beta_3$ integrin activation[24] (inside-out signalling) and P-selectin exposure, a marker for alpha granule secretion. These activation markers were detected using fluorescent antibodies from BD Biosciences; fluorescein isothiocyanate (FITC)-conjugated PAC-1 mAb (PAC-1 clone; 1.25 ng/μL) that recognizes the active conformation of $\alpha_{IIb}\beta_3$, and allophycocyanin (APC)-conjugated anti-CD62P mAb (AK-4 clone; 0.63 ng/μL) for P-selectin. In addition, R-phycoerythrin (PE)-conjugated anti-CD42b mAb (HIP1 clone; 1.25 ng/μL) was used as a platelet identifier for gating. A 10–15 min incubation (room temperature, dark) produced an optimal signal to noise, with this temporal window resulting from continuous droplet formation for a 5 min period required to collect ~100,000 droplet-confined platelets in a tube followed by incubation for 10 min at room temperature. Technical developments are envisaged for continuous encapsulation and continuous platelet release following an in-tubing dynamic incubation to improve the platelet-platelet incubation time reproducibility and allow assay automation. Further assay refinements consider the use of a mineral oil overlay to eliminate, albeit rare, droplet coalescence at the emulsion:air interface. For the larger, 50 μm droplets a 60 min incubation was used to allow aggregation to conclude at room temperature in the absence of stirring (see ESM Fig. 2). This allows biomarker presentation with an appreciable signal to noise.

Platelets were released from the droplets and fixed by breaking the emulsion. This involved removal of the fluoro-oil layer beneath the emulsion layer, the addition of 200 μL CellFix™ fixative (BD Biosciences) then 200 μL 1*H*,1*H*,2*H*,2*H*-perfluoro-1-octanol (PFO, Merck), a weak but neat surfactant that exchanges with the PEG-PFPE surfactant to coalesce the droplets with fixative to promptly preserve platelet activation states. Careful pipetting is then needed to retrieve the platelet volume while avoiding contamination with PFO. As a consequence many platelets are discarded, and this is further exacerbated when using a mineral oil overlay. Nevertheless, the extreme throughput of droplet microfluidics allows 10's of thousands of platelets (from the original 100,000) to be retrieved for analysis. Finally samples were measured using an Accuri C6 cytometer (BD Biosciences). In the case of the minimal collectives, samples were first diluted with PBS to substantially reduce co-incident events during flow cytometry.

The droplet microfluidics approach for capturing intrinsic single platelet sensitivities was test-driven using a CVX dose response experiment. Key data are presented in Figs. 2a and 2b, with vehicle controls compared to maximal stimulations with 100 ng/mL CVX and an intermediate 1 ng/mL CVX stimulation producing a distinct bimodal activation distribution for both $\alpha_{IIb}\beta_3$ active conformation and P-selectin expression level end-points. Results are compared with platelet collectives able to communicate in bulk solution, but otherwise treated to the same methodology as droplet-confined single platelets. The platelet collectives demonstrate substantial (~20-fold) median sensitivity gains. This behaviour can be attributed to hypersensitive platelets (identified by single platelet experiments) activating and coordinating the activation of neighbouring platelets by paracrine signalling. The overall collective dose response behaviour[9] indicates a broad-scale sensitivity continuum (not hetero-

Journal : CMBE MS Code : 12195 PIPS No. : 665 ☐ TYPESET ☑ DISK ☐ LE ☑ CP Dispatch : 13-1-2021 Pages : 8

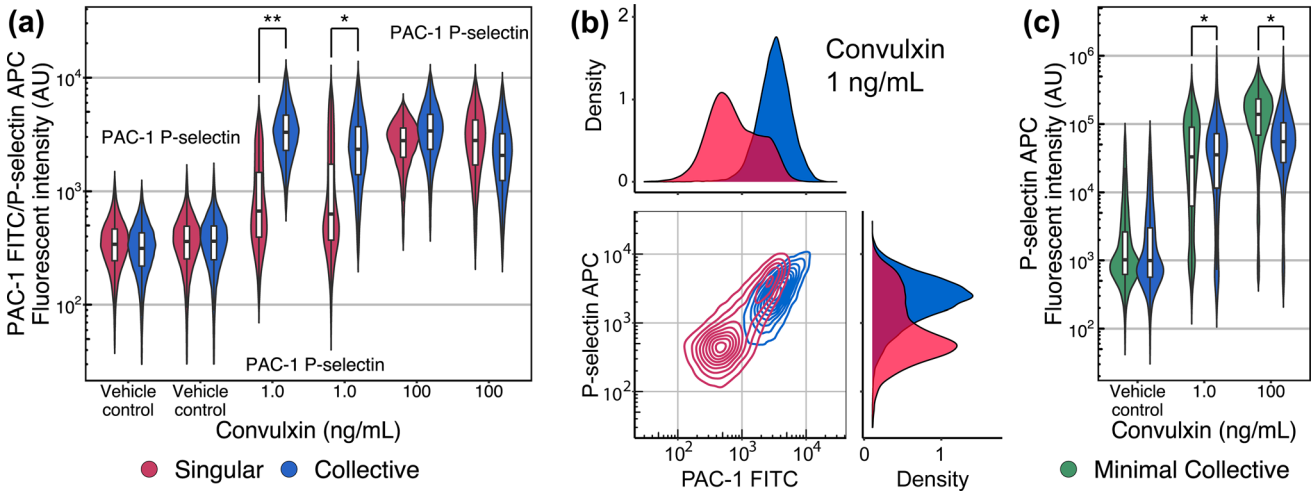

FIGURE 2. ***Single and collective platelet responses to CVX stimulation.*** **Signals from vehicle controls, 1 ng/mL and 100 ng/mL CVX stimulations of single droplet-confined platelets and bulk, platelet collectives, with PAC-1 and P-selectin end-points (a). Contour and density plots of the fully activated collective condition and the bimodal activation distribution of single platelets stimulated with 1 ng/mL CVX (b). Minimal collective (0–15 platelets) and bulk, collective platelet vehicle controls and responses to 1 ng/mL and 100 ng/mL CVX stimulations using the P-selectin end-point (c). The relative risk was used to ascertain significance (*>2, **>10). For single platelet conditions, n = 10,000–36,000 platelet events were measured, and $n \approx$ 40,000–55,000 for the minimal collective and collective conditions. Violins were plotted using the 1–99th percentiles. Figure adapted from Jongen *et al*[9] (CC BY 4.0)**

typic sensitivity states). With low CVX doses (0.1 and 0.3 ng/mL), rare, hyper-reactive platelets drive the activation of some neighbours and with increasing doses progressively more platelets are directly activated by CVX and activate other neighbours until sufficient numbers of platelets are activated to drive the entire population into a fully activated state. Other experimental scenarios and outcomes may indicate the existence of heterotypic populations. However, platelet variability will likely obscure the boundaries between platelet subtypes. In this event, peak fitting software from the field of spectroscopy is well suited for identifying different platelet subtypes within the density plots.

The collective sensitivity gains are attributed to paracrine cross-talk between platelets. Minimal platelet collectives with 0–15 platelets encapsulated within 50-μm-diameter droplets (~65 pL) evidence this inference. The minimal collectives produced platelet population responses similar to platelet collectives (size-based gating was removed to capture platelet aggregates). However, complete activation produced P-selectin expression signals exceeding those of the platelet collectives. This reveals the consequences of confinement, in which secretion products accumulate, driving platelets to higher activation states. With intermediate 1 ng/mL CVX stimulations the P-selectin expression signals span 4 orders of magnitude (see Fig. 2c). This is a result of variable platelet numbers (0–15 platelets), dictated by the Poisson distribution during encapsulation, but also the generation of two population states: by extending analysis to fluorescent imaging using P-selectin and CD42b biomarkers allows the identification of droplets containing aggregates and others with multiple platelets but without aggregates, indicating the presence of hypersensitive platelets in the former but not the latter. These considerations can be tested using experiments involving paracrine inhibitors. Taken, together the data emerging from droplet-confined single platelet and minimal collective measurements holds promise for the development of mathematical models for predicting community cooperation and resultant platelet collective behaviours originating from imbalance in the platelet population structure.

MICROMIXING

Investigating single cell phenotypic diversity demands assay precision and reliability to prevent the population structure from being artificially distorted. For single platelet sensitivity measurements, each platelet must be encapsulated with defined agonist and antibody quantities. While droplet microfluidics represents an appealing route to automation, occasional flow oscillations alter droplet contents (see Fig. 3a). In practice, this requires continuous supervision to discard these droplets from analysis.

As a step towards unattended automation we have integrated a micromixing element for the homogenization of agonist and antibody inputs upstream of

Journal : CMBE MS Code : 12195 PIPS No. : 665 TYPESET DISK LE CP Dispatch : 13-1-2021 Pages : 8

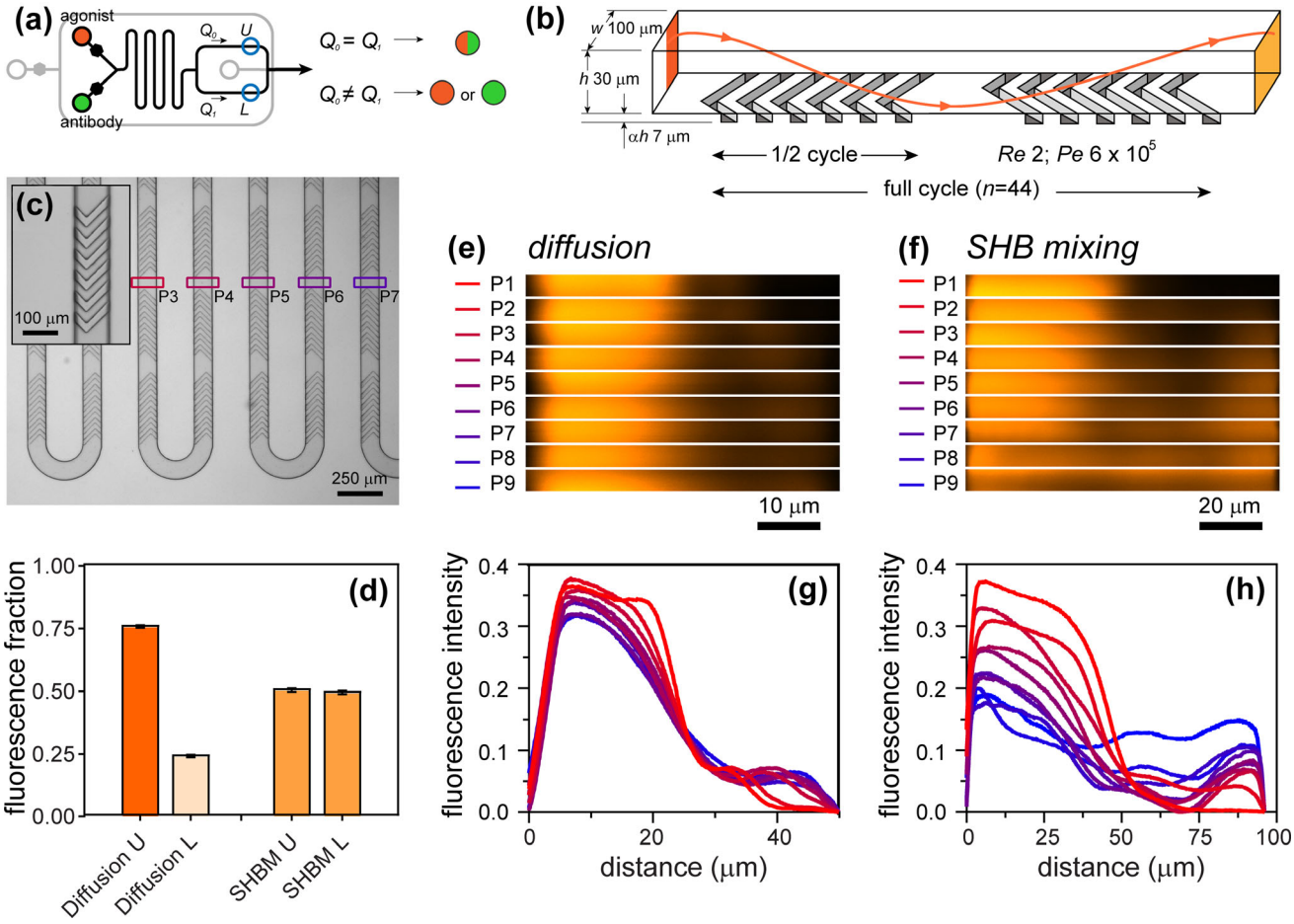

FIGURE 3. ***Staggered herringbone micromixing.*** **Device layout with illustration of flow instability consequences for droplet loading (a). Staggered herringbone (SHB) micromixing concept with flow and mixing conditions (b). SHB microfabricated ridges and distribution within the serpentine channel, with P3–7 indicating fluorescent confocal microscopy measurement positions (c). Fluorescence distributions (mean ± SD, *n* = 3) emerging from the upper (U) and lower (L) outlets (see (a), blue circles) at the end of the serpentine channel for diffusion-limited mixing and SHB micromixing (d). 3D fluorescent cross-sections and intensity profiles of diffusion-limited (e, g) and SHB micromixing (f, h) at the different P1–P9 measurement positions.**

droplet generation to ensure the accurate dosing of each droplet. To this end, we have used topographic patterning in the form of a staggered herringbone (SHB) micromixer[19] (see Fig. 3b). In a first prototype, devices were fabricated to a height of 30 μm, requiring 40 μL/min fluoro-oil, 2μL/min platelets, and 4 μL/min agonist and antibody flows for the reliable production of ~14 pL droplets at ~12 kHz. Herringbone structures in repeats of 6 were alternated in 44 cycles along the 45-mm-long serpentine channel (see Fig. 3c and ESM CAD) and fabricated to a depth of 7 m within the base of the microchannel. The serpentine channel width was increased from 50 to 100 μm producing equivalent Reynolds number ($Re = 2$) and Péclet numbers for the original and herringbone micromixer systems. The mixing performance of lateral diffusion was compared with herringbone-driven micromixing using an experiment combining PBS with a second PBS stream containing 100 μg/mL PLL-FITC (Merck, M_{wt} 50 kDa; $Pe = 6 \times 10^5$) which served as an antibody model with a similar diffusion coefficient ($D = 3 \times 10^8$ cm^2/s). Outputs from either side of the ring structure were measured using a fluorescent plate reader (BMG LabTech FLUOstar Optima).

The herringbone structures introduce asymmetric drag, creating flow anisotropy which results in the lateral circulation and folding of the two input laminar streams.[19] The structures are grouped creating a half cycle to cumulatively drive circulation in one direction, then mirrored for circulation in the opposite direction to complete a cycle. The staggered herringbone micromixer delivered complete mixing, with equivalent PLL-FITC levels delivered to the upper and lower outlets of the ring structure at the end of the serpentine channel. In contrast, diffusion-limited PLL-FITC homogenization produced a 3-fold difference in the PLL-FITC levels (see Fig. 3d). Standard fluorescent imaging was used to compare diffusion-limited

Journal : CMBE MS Code : 12195 PIPS No. : 665 ☐ TYPESET ☑ DISK ☐ LE ☑ CP Dispatch : 13-1-2021 Pages : 8

homogenization with SHB micromixing throughout the 45-mm-length of the serpentine channel (see ESM Fig. 3), corroborating the fluorescent fractions from the upper and lower outputs.

Diffusive transport is slow, whereas SHB micromixing produced layers in the flow. To image PLL-FITC dispersion throughout the serpentine channel cross-section fluorescent confocal microscopy was used (Leica SP8, 5x objective (14x zoom), 0.15 NA, 488 nm excitation, 500–600 nm emission, 0.5 μm z step, 0.28 pinhole). The time dependent PLL-FITC profile for lateral diffusion is compared with SHB micromixing in Figs. 3e–3h. As predicted with diffusion-limited mass transfer, the fluorescent gradient diminishes along the channel. There is also the emergence of a low fluorescent signal at the far side of the channel, perhaps indicating small magnitude secondary Dean flows ($\kappa \approx 0.3$; 150 μm radius of curvature) generated at the 11 hairpins along the serpentine. With the SHB micromixer the PLL-FITC stream is alternately folded, stretching and thinning the fluid layers with diffusion concluding mixing between the narrowing layers. Although mixing is achieved at the outlets, we have incorporated ~3-fold more SHB mixing cycles than used in the first demonstration by Stroock *et al.*[19] We largely attribute this to the lower number of ridges in each of our half cycle patterns ($6 < 10$). Therefore, we predict this prototype can be improved by increasing the herringbone repeats for extensive lateral transport before flow reversal in the following half cycle. In doing so, the serpentine can be shortened to produce a smaller footprint device with lower back pressure and faster flow equilibration. Nevertheless, the current staggered herringbone mixing element ensures accurate reagent dispensing in droplets and can readily be applied to other microfluidic applications requiring on-board mixing.

CONCLUSIONS

In summary, the droplet microfluidics and cytometry workflow provides a high throughput approach for measuring intrinsic platelet functionality. The inclusion of a herringbone micromixer ensures the accurate delivery of agonist and antibody reagents to the droplets and represents a step towards assay automation for reliably profiling platelet functional diversity.

SUPPLEMENTARY INFORMATION

The online version of this article (https://doi.org/10.1007/s12195-020-00665-6) contains supplementary material, which is available to authorized users.

ACKNOWLEDGMENTS

The authors are grateful to the blood donors, and also to George Devitt and Dianne M. Lopez for access to a fluorescent plate reader. The research was funded by Marie Curie (333721, J.W.), the British Heart Foundation (FS/13/67/30473, M.S.A.J.), the National Institute of Health (R01 HL101972) and the Medical Research Council (MC_PC_15078, M.S.A.J.).

AUTHOR CONTRIBUTIONS

MS.A.J., S.I.R.L., P.M.H. and J.W. undertook the research. M.S.A.J., S.I.R.L. and J.W. prepared the figures and manuscript. P.M.H., N.A.E. and O.J.T.M. revised and edited the manuscript. All authors approved the final version of the manuscript.

CONFLICT OF INTEREST

MS.A.J., S.I.R.L., P.M.H., N.A.E., O.J.T.M. and J.W. declare no conflicts of interest.

RESEARCH INVOLVING HUMAN AND ANIMAL RIGHTS

All human subject research was carried out in accordance with institutional guidelines approved by the University of Southampton Ethics Committee ((ERGO 5538) and South Central – Hampshire B National Research Ethics Service (REC: 14/SC/0211)). No animal studies were carried out by the authors for this article.

REFERENCES

[1]Alberio, L., O. Safa, K. J. Clemetson, C. T. Esmon, and G. L. Dale. Surface expression and functional characterization of α-granule factor V in human platelets: effects of ionophore A23187, thrombin, collagen, and convulxin. *Blood*. 95(5):1694–1702, 2000.

[2]Baaten, C. C. F. M. J., H. ten Cate, P. E. J. van der Meijden, and J. W. M. Heemskerk. Platelet populations and priming in hematological diseases. *Blood Rev.* 31(6):389–399, 2017.

[3]Buttarello, M., G. Mezzapelle, F. Freguglia, and M. Plebani. Reticulated platelets and immature platelet fraction: Clinical applications and method limitations. *Int. J. Laboratory Hematol.* 42(4):363–370, 2020.

[4]Clemetson, K. J., and J. M. Clemetson. Platelet collagen receptors. *Thromb. Haemost.* 86(07):189–197, 2001.

[5]Corash, L., H. Tan, and H. R. Gralnick. Heterogeneity of human whole blood platelet subpopulations. I. Relationship between buoyant density, cell volume, and ultrastructure. *Blood* 49(1):71–87, 1977.

[6]Gianazza, E., M. Brioschi, R. Baetta, A. Mallia, C. Banfi, and E. Tremoli. Platelets in healthy and disease states: from biomarkers discovery to drug targets identification by proteomics. *Int. J. Mol. Sci.* 21(12):4541–4584, 2020.

[7]Guo, M. T., A. Rotem, J. A. Heyman, and D. A. Weitz. Droplet microfluidics for high-throughput biological assays. *Lab Chip*. 12(12):2146–2155, 2012.

[8]Holtze, C., A. C. Rowat, J. J. Agresti, J. B. Hutchison, F. E. Angilè, C. H. J. Schmitz, *et al*. Biocompatible surfactants for water-in-fluorocarbon emulsions. *Lab Chip*. 8(10):1632–1639, 2008.

[9]Jongen, M. S. A., B. D. MacArthur, N. A. Englyst, and J. West. Single platelet variability governs population sensitivity and initiates intrinsic heterotypic responses. *Commun. Biol.* 3(1):281, 2020.

[10]Karpatkin, S. Heterogeneity of human platelets: II. Functional evidence suggestive of young and old platelets. *J. Clin. Investig.* 48(6):1083–1087, 1969.

[11]Kroll, M. H., J. D. Hellums, L. V. McIntire, A. I. Schafer, and J. L. Moake. Platelets and shear stress. *Blood*. 88(5):1525–1541, 1996.

[12]Lane, S. I. R., J. Butement, J. Harrington, T. Underwood, J. Shrimpton, and J. West. Perpetual sedimentation for the continuous delivery of particulate suspensions. *Lab Chip*. 19(22):3771–3775, 2019.

[13]Lordan, R., A. Tsoupras, and I. Zabetakis. Platelet activation and prothrombotic mediators at the nexus of inflammation and atherosclerosis: potential role of antiplatelet agents. *Blood Rev*. 2020. https://doi.org/10.1016/j.blre.2020.100694.

[14]Luo, T., L. Fan, R. Zhu, and D. Sun. Microfluidic single-cell manipulation and analysis: Methods and applications. *Micromachines Basel* 10(2):104, 2019.

[15]Margolis, J. Glass surface and blood coagulation. *Nature*. 178(4537):805–806, 1956.

[16]Masters, A., and P. Harrison. Platelet counting with the BD AccuriTM C6 flow cytometer. *Platelets*. 25(3):175–180, 2014.

[17]Munnix, I. C. A., J. M. E. M. Cosemans, J. M. Auger, and J. W. M. Heemskerk. Platelet response heterogeneity in thrombus formation. *Thromb. Haemost.* 102(12):1149–1156, 2009.

[18]Nieswandt, B., and S. P. Watson. Platelet-collagen interaction: is GPVI the central receptor? *Blood.* 102(2):449–461, 2003.

[19]Stroock, A. D., S. K. W. Dertinger, A. Ajdari, I. Mezić, H. A. Stone, and G. M. Whitesides. Chaotic mixer for microchannels. *Science*. 295(5555):647–651, 2002.

[20]Theodoros, G., and C. S. Papaioannou. Vascular wall shear stress: Basic principles and methods. *Hellenic J. Cardiol.* 46:9–15, 2005.

[21]Thompson, C. B., and J. A. Jakubowski. The pathophysiology and clinical relevance of platelet heterogeneity. *Blood*. 72(1):1–8, 1988.

[22]Tremolizzo, L., G. Sala, and C. Ferrarese. Platelet activation. In: Encyclopedia of Psychopharmacology, edited by I. P. Stolerman. Berlin: Springer, 2010, pp. 1034–1035.

[23]Umbanhowar, P. B., V. Prasad, and D. A. Weitz. Monodisperse emulsion generation via drop break off in a coflowing stream. *Langmuir*. 16(2):347–351, 2000.

[24]Watson, S. P., J. M. Auger, O. J. T. McCarty, and A. C. Pearce. GPVI and integrin αIIbβ3 signaling in platelets. *Journal of Thrombosis and Haemostasis*. 3(8):1752–1762, 2005.

Journal : CMBE MS Code : 12195 PIPS No. : 665 ☐ TYPESET ☑ DISK ☐ LE ☑ CP Dispatch : 13-1-2021 Pages : 8